ACS Macro Letters

Letter

pubs.acs.org/macroletters

pH-Responsive Cellulose Nanocrystal Gels and Nanocomposites

Amanda E. Way,[†] Lorraine Hsu,[†] Kadhiravan Shanmuganathan,[†] Christoph Weder,[‡] and Stuart J. Rowan*,[†]

[†]Department of Macromolecular Science and Engineering, Case Western Reserve University, 2100 Adelbert Road, Cleveland, Ohio 44106, United States

[‡]Polymer Chemistry and Materials, Adolphe Merkle Institute, University of Fribourg, Rte de l'Ancienne Papeterie, CH-1723 Marly 1, Switzerland

Supporting Information

ABSTRACT: We show that functionalization of the surface of cellulose nanocrystals (CNCs) with either carboxylic acid (CNC−CO_2H) or amine (CNC−NH_2) moieties renders the CNCs pH-responsive. At low pH, where the amine groups are protonated, CNC−NH_2 forms aqueous dispersions in water on account of electrostatic repulsions of the ammonium moieties inhibiting aggregation. However, a transition to hydrogels is observed at higher pH where the CNC−NH_2 are neutral and the attractive forces based on hydrogen bonding dominate. The opposite behavior is observed for CNC−CO_2H, which are dispersible at high pH and form gels in an acidic environment. We further show that these pH-responsive CNCs can be incorporated into a poly(vinyl acetate) matrix to yield mechanically adaptive pH-responsive nanocomposite films.

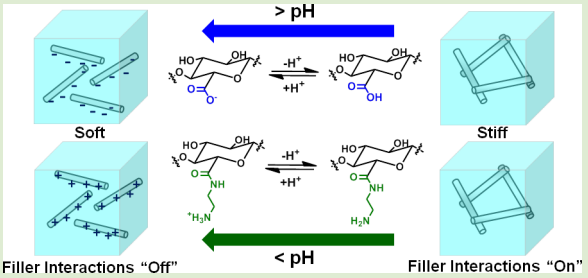

Cellulose nanocrystals (CNCs or cellulose whiskers) are attracting considerable attention as reinforcing fillers in polymer nanocomposites[1−7] and also as interesting nanomaterials in their own right.[8] CNCs are attractive on account of their availability from a variety of renewable biosources, excellent mechanical properties, and low density and have been used as a reinforcing filler for a wide range of polymer matrices.[9−19] They can be isolated from a range of renewable materials including plants, such as cotton,[20] wood,[21] wheat straw,[22] sisal,[23] and sugar beet,[24] bacteria,[25] and sea creatures known as tunicates.[26] Depending on the biosource from which they are obtained, the aspect ratio of CNCs varies from about 10 to 100. One of the attractive features of CNCs is the possibility to tailor their surface properties through functionalization of the surface hydroxyl groups. Several synthetic protocols for surface functionalization have been reported in the literature, primarily with the goal of enhancing the dispersibility of CNCs in solvents and polymer matrices.[27] A common functionalization of CNCs is sulfonation of the surface hydroxyl groups,[28,29] which occurs as a side reaction during the isolation of the CNCs from the appropriate biosource upon hydrolysis with sulfuric acid. The introduction of these negatively charged sulfate groups provides electrostatic repulsion between the CNCs, which aids their dispersion in aqueous and polar organic solvents. If hydrochloric acid is used instead of sulfuric acid for the hydrolysis, uncharged CNCs are obtained, which are generally more difficult to disperse than their charged counterparts.[2] To increase the dispersibility of such CNCs, surface oxidation of the primary alcohols to carboxylic acid moieties[30−34] has been carried out. If deprotonated, the negatively charged carboxylate groups provide for electrostatic repulsion among the nanocrystals, which leads to good dispersibility. Alternatively, grafting of polymers to the surface of CNCs has been used to enhance the stability of CNC suspensions on account of enthalpic as well as entropic effects.[35] The hydrophobicity of CNCs can be dramatically increased through trimethylsilylation[36] or acetylation,[37] which aids dispersion of the CNCs in organic solvents and hydrophobic polymer matrices. Other functionalizations of CNCs include reaction with acid anhydrides[38] and decoration with epoxides via reaction with epichlorohydrin,[39] which can subsequently be ring-opened with ammonium hydroxide to yield amine-functionalized CNCs.

Recently, we have shown that sulfonated CNCs can be used as a stimuli-responsive filler to create mechanically adaptive polymer nanocomposites, in a range of different polymer matrices, which exhibit dramatic stiffness changes when exposed to an aqueous environment.[40−48] It is proposed that the nanocomposite stiffness can be controlled by switching on/off the attractive interactions between the CNCs. In the dry "on" state, strong filler−filler (as well as filler−matrix) interactions exist, which are presumably dominated by hydrogen bonding of the CNC surface hydroxyl groups. This allows stress to be transferred across a rigid, percolating CNC network, resulting in a comparably stiff nanocomposite. Upon exposure to an aqueous environment, water diffuses into the nanocomposite and, aided by electrostatic repulsion of the

Received: June 12, 2012
Accepted: July 16, 2012
Published: July 20, 2012

negatively charged surface sulfate groups, weakens the filler–filler (and filler–matrix) interactions. This results in disengagement of the reinforcing CNC network and softening of the nanocomposite. On the basis of our prior results and with this mechanism in mind, we speculated that it should be possible to alter the surface chemistry of the CNCs so that a more specific stimulus than water can be used to alter the CNC interactions and thus the mechanical properties of their corresponding nanocomposites.

As a first demonstration of this concept, we report, herein, the functionalization of CNCs with groups that are sensitive to pH,[49] namely, carboxylic acid (CNC–CO_2H) and amine (CNC–NH_2) moieties. We show how the pH changes the rheological properties of aqueous dispersions/gels of these pH-sensitive CNCs and introduce pH-responsive nanocomposites made on the basis of these materials, whose mechanical properties can be influenced (in both dry and water swollen states) via the pH.

Figure 1a schematically shows how pH changes should affect the interactions between these CNCs. In an aqueous

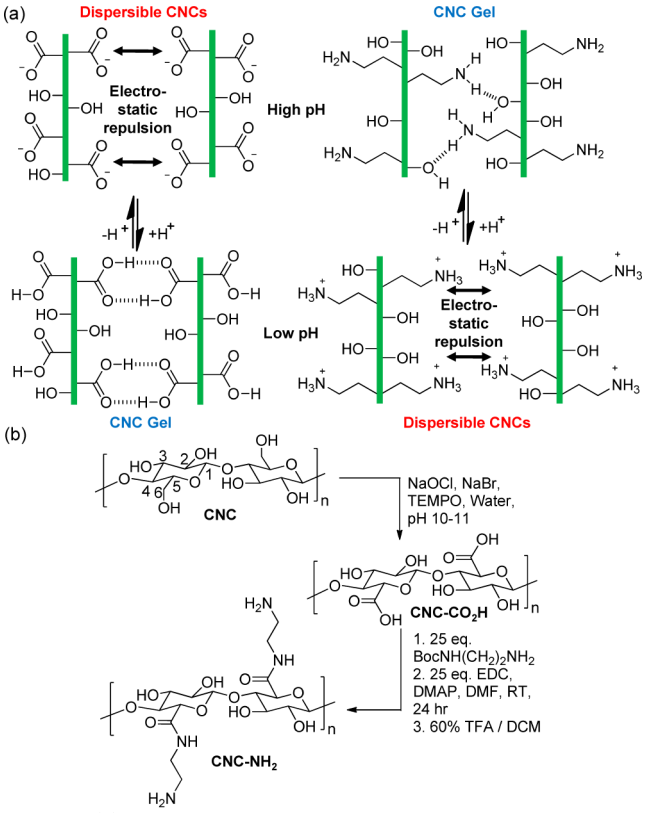

Figure 1. (a) Schematic representation of the proposed interactions between CNC–CO_2H and CNC–NH_2 at high and low pH; (b) Synthesis of CNC–CO_2H and CNC–NH_2 from uncharged CNCs.

environment of high pH, the carboxylated CNCs (CNC–CO_2^-) are deprotonated and negatively charged, and therefore, electrostatic repulsions should significantly reduce the attractive interactions between the CNCs. Conversely, at low pH the carboxylated CNCs are protonated and attractive interactions should occur through hydrogen bonding of the carboxylic acid and hydroxyl moieties. The amine-functionalized CNCs can be expected to behave in an opposite manner, carrying few, if any, charges at high pH, and allowing the CNCs to interact in an attractive manner. At low pH the amines are protonated (CNC–NH_3^+), which should reduce the filler interactions through electrostatic repulsions.

For this study we first isolated non-surface-modified CNCs via hydrochloric acid hydrolysis of the mantles of tunicates using an established protocol.[50] Tunicate CNCs have an aspect ratio of about 80, which is higher than that of CNCs from most other biosources, with dimensions of about 25 nm × 2.2 μm; they exhibit a high stiffness with a tensile modulus of about 140 GPa.[51] The synthetic process for converting the tunicate CNCs into CNC–CO_2H and CNC–NH_2 is shown in Figure 1b (See Supporting Information for experimental details). CNC–CO_2H was prepared in 93% yield via the oxidation of the primary hydroxyl group using literature conditions (NaOCl, TEMPO, and NaBr).[35] Conductometric titrations with sodium hydroxide indicate a carboxylic acid surface functionality of about 1080 mmol/kg (Figure S1 in the Supporting Information).[33] CNC–NH_2 was prepared by reacting CNC–CO_2H with an excess (25 equiv) of mono Boc-protected ethylene diamine using standard peptide coupling techniques (1-ethyl-3-(3-dimethylaminopropyl)carbodiimide (EDC) and 4-dimethylaminopyridine (DMAP)). The surface functionalization of the resulting CNCs was determined by measuring the amount of residual carboxylic acid moieties remaining (ca. 310 mmol/kg) by conductometric titration with sodium hydroxide, suggesting that conversion of about 71% carboxyl groups has been achieved. The Boc-protected-amine CNCs were subsequently exposed to TFA/DCM to remove the protecting group and yield the amine-functionalized CNCs. Assuming complete cleavage of the Boc-protecting group, the amine functionalized CNCs have about 770 mmol/kg of amine groups and about 310 mmol/kg of carboxylic acid moieties on the surface. Thus, at neutral pH, where both these functionalities are expected to be in their ionized state, these CNCs have an overall positive charge of about 460 mmol/kg. The comparison of the transmission electron micrographs of CNC–CO_2H (Figure 2a) and CNC–NH_2 (Figure 2b) shows that the

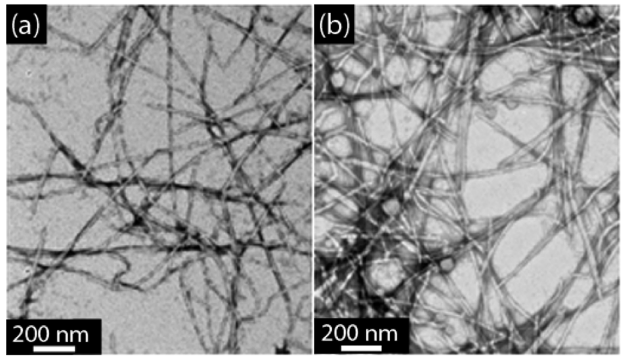

Figure 2. Transmission electron micrographs of (a) CNC–CO_2H and (b) CNC–NH_2. To prepare the samples, 0.1 wt % aqueous CNC dispersions (pH 7) were drop-cast on carbon-coated copper grids and stained with 2% uranyl acetate. The average thickness of the CNCs is 22.5 ± 5.0 nm (CNC–CO_2H) and 23 ± 4.8 nm (CNC–NH_2).

functionalization did not significantly affect the dimensions of the CNCs. FT-IR spectra were recorded to confirm the functionality present on the surface of the CNCs (Figure S2 in the Supporting Information). The IR spectrum of a dry CNC–CO_2H sample cast from acidic solution (pH 3) shows a peak at about 1702 cm^{-1}, consistent with the C=O stretch of a carboxylic acid moiety. The IR spectrum of a sample cast from

dx.doi.org/10.1021/mz3003006 | ACS Macro Lett. 2012, 1, 1001–1006

basic solution (pH 11), by contrast, shows the carbonyl peak at about 1616 cm^{-1} consistent with the presence of carboxylate ions. The CNC−NH_2 FT-IR spectra show the carbonyl peak at about 1633 cm^{-1}, irrespective of the pH of the solutions from which the sample was cast, consistent with the formation of the expected amide.

To show how the pH affects the properties of these CNCs, a series of aqueous dispersions containing 2.7 wt % of the functionalized CNCs with a pH ranging from 1 to 11 was prepared. This was achieved by using HCl or NH_4OH to adjust the pH of water CNC dispersions to 1, 3, 5, 7, 9, or 11 (all dispersions were diluted by a negligible amount). Transmission electron microscopy (TEM) images of CNC−CO_2H and CNC−NH_2 indicate that the structure of the CNCs was not significantly affected by exposure to acid or base (Figure S3 in the Supporting Information) in the time frame required to carry out the rheological characterization (ca. 1 h). Gratifyingly, at different pH the aqueous dispersions of the two functionalized CNCs showed dramatic visual differences (Figure 3a)

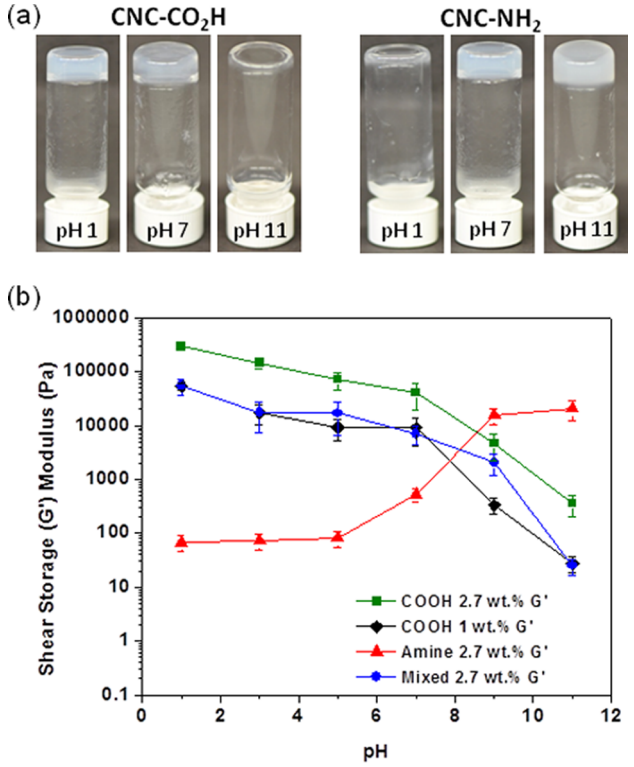

Figure 3. (a) Images of aqueous dispersions of 2.7 wt % CNC−CO_2H and 2.7 wt % CNC−NH_2 at pH 1, 7, and 11; (b) Summary of the shear storage modulus at different pH of the 2.7 wt % CNC−CO_2H (green squares), 1 wt % CNC−CO_2H (black diamonds), 2.7 wt % CNC−NH_2 (red triangles), and a mixture of 0.75 wt % CNC−CO_2H and 2.0 wt % CNC−NH_2 (blue circles). Shear moduli at 1 Hz (6.28 rad/s) were obtained from frequency sweep experiments (see Supporting Information, Figures S5−S6) averaged over three samples.

that are consistent with the expected behavior as shown schematically in Figure 1. The carboxylated CNCs form gels at low pH, consistent with the formation of a percolating network of interacting CNC fibers. At high pH, however, these gels transform into free-flowing dispersions, consistent with electrostatic repulsions of charged CNC−CO_2^-, which disrupts the nanofiber network. On the other hand, the amine-functionalized CNCs form gels at high pH and low-viscosity dispersions at low pH. Oscillatory rheology shear experiments were carried out to examine these materials in more detail. As can be seen from the data in Figure 3b, the shear storage modulus (G') of an aqueous dispersion containing 2.7 wt % of the carboxylated CNCs increases from about 350 Pa at pH 11 to 290000 Pa at pH 1, where the material forms a gel. Conversely, the G' of a mixture of 2.7 wt % of amine CNCs in water decreases from about 21000 Pa at pH 11 to about 65 Pa at pH 1. Figure 3b shows that the modulus of the amine gels decreases significantly when the pH is lowered to below 9, consistent with a change in the charge of the CNCs (i.e., deprotonation of the ammonium ions) in a regime that is commensurate with the pK_a of primary ammonium ions (∼9−10).[52] A plot of G' and G'' of the samples versus pH shows that $G' > G''$ (an estimation of the gel point) above a pH of about 6 (see Figures S4 and S5 in Supporting Information). A more gradual change in the rheological properties is observed with pH in the case of the CNC−CO_2H. Interestingly, the modulus only shows a significant drop above a pH of ca. 7 and $G' > G''$ at a pH ≤ 9 (see Figures S4 and S5 in Supporting Information). Thus, the dispersion occurs at a higher pH value than might be expected based on the pK_a of a carboxylic acid (ca. 4.5).[53] This behavior may hint at the formation of multiple carboxylic acid hydrogen bonded dimers (Figure 1) between the CNCs, which would stabilize the carboxyl group in its protonated state. Nonetheless the trend is clear, and strong interacting networks are formed when the CNCs are either uncharged or weakly charged and dispersions are formed with highly charged CNCs.

It is worthy to note that the modulus of the CNC−CO_2H gel (ca. 290000 Pa at pH 1) is significantly higher than that of the CNC−NH_2 gel (ca. 21000 Pa at pH 11), which could be the result of the stronger interactions of the carboxylic acid dimers versus the amine hydrogen bonding interactions. However, it could also be related to the fact that CNC−NH_2 has residual carboxylate groups on its surface and as such will be slightly negatively charged at high pH. We also investigated the properties of a 1 wt % dispersion of CNC−CO_2H, which has the same overall charge density (as opposed to the same weight content of CNCs) as the 2.7 wt % CNC−NH_2 dispersion (see Figure S4 in Supporting Information for frequency sweep experiments). As can be seen from the data shown in Figure 3b, this system follows the same trend as the 2.7 wt % CNC−CO_2H dispersions but exhibits a lower modulus over the pH range. This composition shows a modulus increase from about 4 Pa at pH 11 to about 54000 Pa at pH 1. The comparison of the G' and G'' modulus data versus pH also indicates a gel point at a lower pH (∼7) than is observed for the higher concentration CNC−CO_2H dispersions. Finally, a 1:1 mixed dispersion of CNC−CO_2H and CNC−NH_2 based on surface charge (0.75 wt % CNC−CO_2H and 2 wt % CNC−NH_2) was prepared. Interestingly, this system showed the same overall trend as the CNC−CO_2H dispersions alone (Figure 3b), which is consistent with the interpretation that CNC−CO_2H forms stronger nanofiber−nanofiber interactions than CNC−NH_2. A comparison of the storage (G') and loss (G'') moduli of this system puts the gel point around pH 7.5.

To explore if the pH-responsive behavior of these CNCs could be imparted to polymer nanocomposites made with these fillers, we prepared CNC−CO_2H and CNC−NH_2 nanocomposites with poly(vinyl acetate) (PVAc). We have previously shown that PVAc nanocomposites with sulfonated CNCs can be mechanically switched with the addition of water.[40−44] Nanocomposites of PVAc containing 10 wt %

dx.doi.org/10.1021/mz3003006 | ACS Macro Lett. 2012, 1, 1001−1006

Table 1. Wet Modulus, Swelling, and Dry Modulus Values for CNC−CO_2H and CNC−NH_2 PVAc Nanocomposites at pH 3, 7, and 11

		wet modulus/MPa (swelling/%)			dry modulus (MPa)		
pH		3	7	11	3	7	11
CNC−CO_2H	22 °C	100 ± 15 (30 ± 3)	60 ± 12 (39 ± 3)	40 ± 8 (64 ± 3)	3850 ± 370	3550 ± 300	2340 ± 152
	37 °C	35 ± 10 (47 ± 3)	20 ± 5 (62 ± 3)	8 ± 2 (85 ± 3)			
	80 °C				290 ± 65	110 ± 25	80 ± 15
CNC−NH_2	22 °C	34 ± 8 (85 ± 4)	51 ± 10 (45 ± 2)	88 ± 21 (27 ± 2)	1230 ± 216	1730 ± 342	2710 ± 432
	37 °C	4 ± 1 (96 ± 4)	11 ± 2 (52 ± 3)	28 ± 8 (38 ± 3)			
	80 °C				21 ± 8	44 ± 15	52 ± 23

CNC−CO_2H or CNC−NH_2 were made via solution-casting from DMF and subsequent vacuum drying. The resulting materials were compression-molded at 85 °C and 3000 psi for 2 min to result in films of a thickness between 300 and 400 μm. The films were placed in acidic, neutral, and basic aqueous solutions of pH 3, 7, and 11 for 3 days before being placed in dynamic mechanical analyzer equipped with an a submersion chamber containing an aqueous solution of the same pH. This procedure allowed the accurate determination of the wet-state modulus of the nanocomposites as a function of pH. As can be seen from the data shown in Table 1 and Figure 4a, the new nanocomposites do indeed show pH-dependent mechanical properties. The tensile storage moduli E' in the wet state were recorded at 22 °C (i.e., near the glass transition temperature (T_g) of water-swollen PVAc (ca. 20 °C[40]) and at 37 °C (i.e., at physiological temperature and well above the T_g of water-swollen PVAc). The wet modulus of the CNC−CO_2H composites increases from 8 MPa at pH 11 to 35 MPa at pH 3 at 37 °C and from about 40 MPa at pH 11 to about 100 MPa at pH 3 at 22 °C (Table 1). These trends mirror those seen in solution and are consistent with the proposed mechanism that the CNC−CNC interactions are changed on account of pH-controlled surface charge density variation. We note that the aqueous swelling of the PVAc/CNC−CO_2H nanocomposites decreases with pH (85, 62, and 47 wt % swelling at pH 11, 7, and 3, respectively, at 37 °C), consistent with charge neutralization and the formation of a CNC network at low pH. The wet moduli of the CNC−NH_2 nanocomposites show an opposite trend and increase as the pH increases, for example, from 4 MPa at pH 3 to 28 MPa at pH 11 at 37 °C and from 34 MPa at pH 3 to 88 MPa at pH 11 at 22 °C. The CNC−NH_2 nanocomposites also swell in the presence of water to a larger degree at a pH where the CNC surface is charged (with 38, 52, and 96 wt % swelling at pH 11, 7, and 3, respectively, at 37 °C). Thus, in both systems the degree of aqueous swelling and the tensile modulus of the nanocomposite films is strongly dependent on the charge density of the CNCs, which as shown can be controlled by way of changing the pH of the surrounding medium.

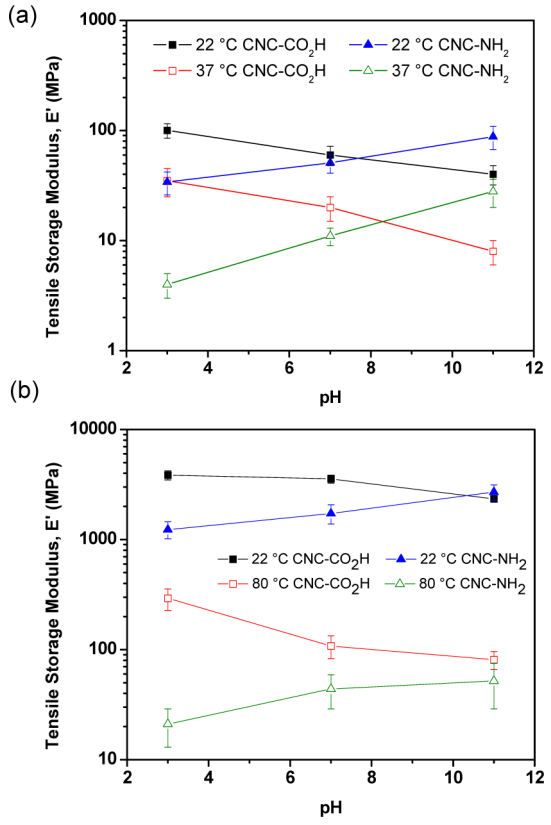

Figure 4. Tensile storage moduli E' of CNC−CO_2H/PVAc and CNC−NH_2/PVAc nanocomposites (10 wt % nanofiller) exposed to aqueous solutions of pH 3, 7, and 11. (a) Moduli were recorded by submersion DMA in the wet state at 22 and 37 °C. (b) Moduli were recorded at 22 and 80 °C after drying the samples. All experiments are averaged over three samples.

To explore to what extent the mechanical properties of such nanocomposites can be influenced on the basis of changing supramolecular interactions (and not on account of or with contribution from different levels of aqueous swelling) the nanocomposite samples conditioned at different pH values were dried (air drying for 2 days and subsequent vacuum drying for 3 days at 60 °C) and their mechanical properties were examined in the dry state. DMA temperature sweeps (Figure S6 in Supporting Information) were conducted between 15 - 90 °C (at 0.1% strain and a fixed frequency of 1 Hz) and the tensile storage moduli E' at 22 °C (well below the T_g of the PVAc nanocomposites (40−60 °C)[40]) and at 80 °C (well above the T_g) are shown in Table 1 and Figure 4b. Gratifyingly, the data match the trends observed for the wet samples. In the case of the 10 wt % CNC−CO_2H nanocomposites, E' increases when the pH is decreased, from 2340 (pH 11) to 3850 MPa (pH 3) at 22 °C and from 80 (pH 11) to 290 MPa (pH 3) at 80 °C. Conversely, E' of the 10 wt % CNC−NH_2 nanocomposites decreases when the pH is decreased from 2710 (pH 11) to 1230 MPa (pH 3) at 22 °C and from 52 (pH 11) to 21 MPa (pH 3) at 80 °C. The weaker reinforcement exhibited by the CNC−NH_2 is consistent with the formation of a weaker reinforcing percolating network as was observed for the aqueous gels formed by these nanofillers. Furthermore, the smaller change in mechanical properties of the CNC−NH_2 nanocomposites with pH is consistent with the fact that the CNC−NH_2 also contain some residual CO_2H functionality on

dx.doi.org/10.1021/mz3003006 | ACS Macro Lett. 2012, 1, 1001−1006

their surface and, therefore, will be charged (albeit to different degrees) at both pH 3 and 11. Importantly, the observed stiffness changes in the dry nanocomposites (where the degree of water swelling is not a complicating factor) are of a significant magnitude (i.e., E' changes by a factor of 2−3), suggesting that the change in surface charge as a consequence of pH exposure has indeed a significant influence on the mechanical properties of these nanocomposites. We note that a small change in T_g with pH exposure is observed (Figure S7 in Supporting Information); the tan δ curves from the DMA temperature sweeps of the dry nanocomposites indicate an increase in T_g with a decrease in pH for the CNC−CO_2H nanocomposites (38 °C at pH 11, 40 °C at pH 7, and 44 °C at pH 3) and the opposite trend being observed for the CNC−NH_2 nanocomposites (48 °C at pH 11, 46 °C at pH 7, and 40 °C at pH 3). This pattern is consistent with the interpretation that uncharged CNCs interact more strongly with the matrix as well as with other CNCs, which results in an increase in T_g. It should be noted that no significant hydrolysis of the PVAc matrix was observed during this process (see Figure S8 in Supporting Information).

In conclusion, we have shown that altering the surface chemistry of CNCs allows access to pH-switchable mechanically adaptable aqueous dispersions and nanocomposites. CNCs functionalized with carboxylic acids (CNC−CO_2H) exhibit an increase in modulus at low pH, while amine-functionalized CNCs (CNC−NH_2) show the opposite behavior. In both cases, the neutral or little charged CNCs show better mechanical reinforcement than their highly charged counterparts. Thus, we demonstrate for the first time that it is possible to alter the surface chemistry of the CNCs and therefore change the stimulus that can be used to alter the CNC interactions and thus the mechanical properties of their corresponding suspensions, gels, and nanocomposites. This ability to reprogram the stimulus that these dynamic nanocomposites are responsive to, by simple surface functionalization of the CNCs, offers the exciting opportunity to access a range of designed mechanically adaptable materials that are sensitive to a specific desired stimulus.

■ ASSOCIATED CONTENT

Supporting Information

Experimental section detailing the isolation and synthesis of the functionalized CNC and the preparation and characterization of the CNC dispersion/gels and PVAc nanocomposites, along with TEM images, FT-IR spectra, rheology data, and DMA data not presented in the paper (Figures S1−S8). This information is available free of charge via the Internet at http://pubs.acs.org/journal/amlccd.

■ AUTHOR INFORMATION

Corresponding Author

*E-mail: stuart.rowan@case.edu.

Notes

Notes. The authors declare no competing financial interest. The authors declare no competing financial interest.

■ ACKNOWLEDGMENTS

The authors gratefully acknowledge financial support from the National Science Foundation under Grant Nos. CBET-0828155, DMR-0804874, and DMR-1204948, the Swiss National Science Foundation (NRP 62: Smart Materials, Nr. 406240_126046), the Lubrizol Corporation, and the Adolphe Merkle Foundation.

■ REFERENCES

(1) Eichhorn, S. J.; Dufresne, A.; Aranguren, M.; Marcovich, N. E.; Capadona, J. R.; Rowan, S. J.; Weder, C.; Thielemans, W.; Roman, M.; Renneckar, S.; Gindl, W.; Veigel, S.; Keckes, J.; Yano, H.; Abe, K.; Nogi, M.; Nakagaito, A. N.; Mangalam, A.; Simonsen, J.; Benight, A. S.; Bismarck, A.; Berglund, L. A.; Peijs, T. *J. Mater. Sci.* **2010**, *45*, 1−33.
(2) Azizi Samir, M. A. S.; Alloin, F.; Dufresne, A. *Biomacromolecules* **2005**, *6*, 612−619.
(3) Habibi, Y.; Lucia, L. A.; Rojas, O. J. *Chem. Rev.* **2010**, *110*, 3479−3500.
(4) Duran, N.; Lemes, A. P.; Duran, M.; Freer, J.; Baeza, J. *J. Chil. Chem. Soc.* **2011**, *56*, 672−677.
(5) Siró, D. Plackett *Cellulose* **2010**, *17*, 459−494.
(6) Ben Azouz, K.; Ramires, E. C.; Van den Fonteyne, W; El Kissi, N.; Dufresne, A. *ACS Macro Lett.* **2012**, *1*, 236−240.
(7) Ma, H.; Burger, C.; Hsiao, B. S.; Chu, B. *ACS Macro Lett.* **2012**, *1*, 723−726.
(8) For some recent examples see; (a) Csoka, L.; Hoeger, I. C.; Rojas, O. J.; Peszlen, I.; Pawlak, J. J.; Peralta, P. N. *ACS Macro Lett.* **2012**, *1*, 867−870. (b) Uetani, K.; Yano, H. *ACS Macro Lett.* **2012**, *1*, 651−655. (c) Padalkar, S.; Capadona, J. R.; Rowan, S. J.; Weder, C.; Won, Y. H.; Stanciu, L. A.; Moon, R. J. *J. Mater. Sci.* **2011**, *46*, 5672−5679. (d) Padalkar, S.; Capadona, J. R.; Rowan, S. J.; Weder, C.; Won, Y. H.; Stanciu, L. A.; Moon, R. J. *Langmuir* **2010**, *26*, 8497−8502.
(9) Favier, V.; Canova, G. R.; Cavaille, J. Y.; Chanzy, H.; Dufresne, A.; Gathier, C. *Polym. Adv.Tech* **1995**, *6*, 351−355.
(10) Ljungberg, N.; Cavaillé, J.-Y.; Heux, L. *Polymer* **2006**, *47*, 6285−6292.
(11) Nakagaito, A. N.; Fujimura, A.; Sakai, T.; Hama, Y.; Yano, H. *Compos. Sci. Technol.* **2009**, *69*, 1293−1297.
(12) Wu, Q. J.; Henriksson, M.; Liu, X.; Berglund, L. A. *Biomacromolecules* **2007**, *8*, 3687−3692.
(13) Schroers, M.; Kokil, A.; Weder, C. *J. Appl. Polym. Sci.* **2004**, *93*, 2883−2888.
(14) Nogi, M.; Yano, H. *Adv. Mater.* **2008**, *20*, 1849−1852.
(15) Nogi, M.; Iwamoto, S.; Nakagaito, A.; Yano, H. *Adv. Mater.* **2009**, *21*, 1595−1598.
(16) Williams, A.; Ibrahim, I. T. *Chem. Rev.* **1981**, *81*, 589−636.
(17) Mohanty, A. K.; Misra, M.; Hinrichsen, G. *Macromol. Mater. Eng.* **2000**, *276*, 1−24.
(18) Svagan, A. J.; Samir, M.; Berglund, L. A. *Biomacromolecules* **2007**, *8*, 2556−2563.
(19) Henriksson, M.; Berglund, L. A.; Isaksson, P.; Lindstrom, T.; Nishino, T. *Biomacromolecules* **2008**, *9*, 1579−1585.
(20) Fleming, K.; Gray, D.; Prasannan, S.; Matthews, S. *J. Am. Chem. Soc.* **2000**, *122*, 5224−5225.
(21) Woodhams, R. T.; Thomas, G.; Rodgers, D. K. *Polym. Eng. Sci.* **1984**, *24*, 1166−1171.
(22) Helbert, W.; Cavaille, J. Y.; Dufresne, A. *Polym. Compos.* **1996**, *17*, 604−611.
(23) Siqueira, G.; Bras, J.; Dufresne, A. *Biomacromolecules* **2009**, *10*, 425−432.
(24) Azizi Samir, M. A. S.; Alloin, F.; Paillet, M.; Dufresne, A. *Macromolecules* **2004**, *37*, 4313−4316.
(25) Grunert, M.; Winter, W. T. *J. Polym. Environ.* **2002**, *10*, 27−30.
(26) Angles, M. N.; Dufresne, A. *Macromolecules* **2000**, *33*, 8344−8353.
(27) Zhou, Q.; Brumer, H.; Teeri, T. T. *Macromolecules* **2009**, *42*, 5430−5432.
(28) van den Berg, O.; Capadona, J. R.; Weder, C. *Biomacromolecules* **2007**, *8*, 1353−1357.
(29) Araki, J.; Wada, M.; Kuga, S.; Okano, T. *Colloids Surf. A* **1998**, *142*, 75−82.
(30) Isogai, A.; Kato, Y. *Cellulose* **1998**, *5*, 153−164.
(31) Davis, N. J.; Flitsch, S. L. *Tetrahedron Lett.* **1993**, *34*, 1181−1184.

(32) de Nooy, A. E.; Besemer, A. C.; van Bekkum, H.; van Dijk, J. A. P. P.; Smit, J. A. M. *Macromolecules* **1996**, *29*, 6541−6547.
(33) da Silva Perez, D.; Montanari, S.; Vignon, M. R. *Biomacromolecules* **2003**, *4*, 1417−1425.
(34) Ma, H.; Hsiao, B. S.; Chu, B. *ACS Macro Lett.* **2012**, *1*, 213−216.
(35) Araki, J.; Wada, M.; Kuga, S. *Langmuir* **2001**, *17*, 21−27.
(36) Grunert, M.; Winter, W. T. *J. Polym Environ.* **2002**, *10*, 27−30.
(37) Habibi, Y.; Chanzy, H.; Vignon, M. R. *Cellulose* **2006**, *13*, 679−687.
(38) Yuan, H.; Nishiyama, Y.; Wada, M.; Kuga, S. *Biomacromolecules* **2006**, *3*, 696−700.
(39) Dong, S.; Roman, M. *J. Am. Chem. Soc.* **2007**, *129*, 13810−13811.
(40) Capadona, J. R.; Shanmuganathan, K.; Tyler, D. J.; Rowan, S. J.; Weder, C. *Science* **2008**, *319*, 1370−1374.
(41) Capadona, J. R.; Shanmuganathan, K.; Trittschuh, S.; Seidel, S.; Rowan, S. J.; Weder, C. *Biomacromolecules* **2009**, *10*, 712−716.
(42) Shanmuganathan, K.; Capadona, J. R.; Rowan, S. J.; Weder, C. *Prog. Polym. Sci.* **2010**, *35*, 212−222.
(43) Shanmuganathan, K.; Capadona, J. R.; Rowan, S. J.; Weder, C. *J. Mater. Chem.* **2010**, *20*, 180−186.
(44) Shanmuganathan, K.; Capadona, J. R.; Rowan, S. J.; Weder, C. *Appl. Mater. Interfaces* **2010**, *2*, 165−174.
(45) Dagnon, K. L.; Shanmuganathan, K.; Weder, C.; Rowan, S. J. *Macromolecules* **2012**, *45*, 4707−4715.
(46) Hsu, L.; Weder, C.; Rowan, S. J. *J. Mater. Chem.* **2011**, *21*, 2812−2822.
(47) Mendez, J.; Annamalai, P. K.; Eichhorn, S. J.; Rusli, R.; Rowan, S. J.; Weder, C. *Macromolecules* **2011**, *44*, 6827−6835.
(48) For an alternative approach to water responsive mechanically adaptable nanocomposites see: Stone, D. A.; Wanasekara, N. D.; Jones, D. H.; Wheeler, N. R.; Wilusz, E.; Zukas, W.; Wnek, G. E.; Korley, L. T. J. *ACS Macro Lett* **2012**, *1*, 80−83.
(49) For examples of pH-sensitive carbon nanotubes and composites see (a) Etika, K. C.; Cox, M. A.; Grunlan, J. C. *Polymer* **2010**, *51*, 1761−1770. (b) Saint-Aubin, K.; Poulin, P.; Saadaoui, H.; Maugey, M.; Zakri, C. *Langmuir* **2009**, *25*, 13206−132011. (c) Grunlan, J. C.; Liu, L.; Regev, O. *J. Colloid Interface Sci.* **2008**, *317*, 346−349. (d) Barone, P. W.; Strano, M. S. *Angew. Chem., Int. Ed.* **2006**, *45*, 8138−8141. (e) Grunlan, J. C.; Liu, L.; Kim, Y. S. *Nano Lett.* **2006**, *6*, 911−915.
(50) Belton, P. S.; Tanner, S. F.; Cartier, N.; Chanzy, H. *Macromolecules* **1989**, *22*, 1615−1617.
(51) (a) Sturcova, A.; Davies, J. R.; Eichhorn, S. J. *Biomacromolecules* **2005**, *6*, 1055−1061. (b) Kimura, F.; Kimura, T.; Tamura, M.; Hirai, A.; Ikuno, M.; Horii, F. *Langmuir* **2005**, *21*, 2034−2037.
(52) Genco, T.; Zemljič, L. F.; Bračič, M.; Stana-Kleinschek, K.; Heinze, T. *Macrom. Chem. Phys.* **2012**, *213*, 539−548.
(53) Orelman, H.; Filpponen, I.; Johansson, L.-S.; Laine, J.; Rojas, O. J. *Biomacromolecules* **2011**, *12*, 4311−4318.